Multipath reduction for bathymetry using adaptive beamforming

Ann E. A. Blomberg
University of Oslo, Norway
Email: aeblombe@ifi.uio.no

Michael Hayes
University of Canterbury, New Zealand
Email: michael.hayes@canterbury.ac.nz

***Abstract*—In this paper we consider adaptive beamforming techniques to suppress the dominant multipath for a multi-element interferometric synthetic aperture sonar. We use a broadband variant of the minimum variance (MV) beamformer and apply it to reconstruct bathymetry using data from the KiwiSAS-4 sonar. This has three vertically displaced hydrophone arrays. The MV beamformer is used to estimate the angle of arrival of the backscattered echo from the sea floor, and from that the height of the sea floor. The conventional delay-and-sum (DAS) beamformer is used for comparison.**

I. Introduction

Accurate high-resolution height maps of the sea floor are of importance in a number of scenarios such as navigation, planning of oil rigs and other sub-sea structures, and recognition of objects on the sea floor. Synthetic aperture side-scan sonars have become a mature technology for high-resolution sea floor imagery [1]. These have been augmented with additional vertically displaced hydrophone arrays to create interferometric synthetic aperture sonars (InSAS). From time of arrival differences between the vertically displaced hydrophones, the echo arrival angle and thus the scatterer height at a given range can be estimated. However, this is predicated on a single echo arriving at each range and this assumption is violated when there are multiple echoes due to sea-surface multipath effects [2].

Another limitation of the two-element interferometer is the lack of resolving capability in the elevation dimension, resulting in *layover* effects in areas with large height variations [3]. Multi-look interferometry has been proposed to overcome this challenge by offering lateral resolution capabilities [4]. Still, the assumption of a single echo impinging on the array at any instant is violated due to multipath propagation.

The effect of sea-surface multipath is to produce delayed replicas of the sea floor scattering; these appear as *ghosts* in the image. Usually these ghosts are more blurred due to a lower ping to ping coherence for the echoes scattered from a moving sea-surface. The strongest of the multipath echoes has a single reflection from the sea surface; this has well separated angle arrival from the direct echo. Unfortunately, the high-order multipaths have arrival angles similar to the direct echo and can only be suppressed by projecting different frequency bands across the swath [5] or perhaps by advanced modeling given accurate bathymetry.

Adaptive beamforming has been used for decades in passive sonar systems for, e.g., improved direction of arrival estimates. Adaptive methods offer improved resolution and better sidelobe suppression compared to conventional beamforming methods. They also have the desired ability to cancel interfering sources by placing a deep null in the beampattern, in the direction of the interfering source.

In [4], Lombardini et. al. suggest applying adaptive beamforming techniques to reflectivity estimation in radar imaging to reduce layover effects. They use a multi-look approach which enables them to resolve scatterers within the same range cell but with different angles of arrival. In 2005, Zerr et. al. applied adaptive beamforming to a sidescan sonar system targeted toward Rapid Environment Assessment [6]. Their results indicated that adaptive beamforming techniques gave similar results to an interferometric approach for direction of arrival estimation.

In this paper we present a method for improved bathymetry estimation using the minimum variance (MV) adaptive beamformer. The MV beamformer was originally developed for a narrowband scenario, but in this work we have extended it to the broadband case by splitting the received signal into frequency bands and processing each frequency band separately. Results from Kiwisas-4 are presented and compared to the conventional delay and sum beamformer.

We start by presenting some of the basic concepts of bathymetry and the issues caused by multipath propagation in Section II. The beamforming techniques which we use are described in Section III. The conventional delay-and-sum (DAS) beamformer and the adaptive MV beamformer are defined first in terms of a narrowband assumption and then extended to the broadband case using a filterbank approach. Our approach to beam steering and selection is also described in this section. Reconstructed bathymetry and SAS-reconstructed images are presented in Section IV and discussed in Section V.

II. Multipath propagation and bathymetry

In this section we introduce the concepts of sea-surface multipath and bathymetric measurements of the seafloor height using a three-element vertical hydrophone array.

A. Sea-surface multipath

One of the major sources of noise and image artefacts in sonar imaging is caused by multipath propagation. While some of the backscattered energy from a target will take the

978-1-4244-5222-4/10/$26.00 ©2010 CROWN

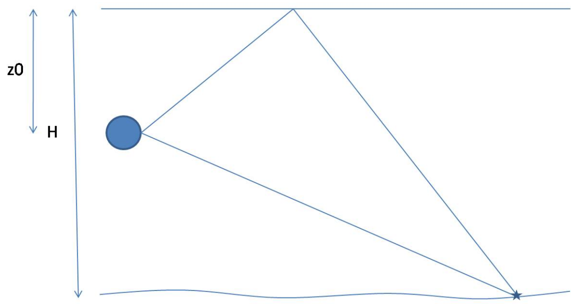

Fig. 1. Sonar geometry showing both the (desired) direct path and the 1st order sea-surface multipath.

direct path back to the receiver, it may also take alternative paths, bouncing one or several times off the sea-surface before reaching the receiver some time after the desired direct path signal. The dominating multipath contribution is often the first order sea-surface multipath, illustrated by Figure 1. Multipath propagation implies that at any instant there may be one or more undesired signals impinging on the array, in addition to the desired signal.

B. Bathymetric measurements using a three-element vertical array

Using an array of two or more vertical elements, bathymetric images of the sea floor may be reconstructed [7]. The difference in time delay (or phase delay in the narrowband case) between the elements is used to estimate the angle of arrival of the plane wave impinging on the array, which again gives an estimate of the height of the scatterer relative to the position of the sonar. When using an array consisting of more than two vertically displaced elements, a multibaseline interferometer may be constructed. Although the multibaseline interferometer reduces noise and adds robustness to the bathymetric images by taking advantage of the redundancy of information, the single echo assumption is still violated in the case of multipath propagation [8] .

In this paper we investigate how conventional and adaptive beamforming techniques may be applied to a three-element vertical array for bathymetry estimation.

III. BEAMFORMING

Having an array consisting of several sensors, beamforming may be used to control the response of the array, or to “form” the beam, either on transmission or on reception, or both. In the case of sidescan sonar used for bathymetry, beamforming may be used to steer the transmitted beam at a given depression angle and also steer the received beam in the expected direction of arrival of the desired echo. The process of beamforming involves both applying a time delay (or a phase delay if the signals are narrowband) and applying apodization weights to each of the sensors. In conventional, non-adaptive beamformers such as the delay-and-sum (DAS) beamformer, the apodization weights are pre-defined and thus data-independent. Often, the sensor weights are defined by a window function, such as a Hann or a Kaiser window, to tailor the beampattern.

A. Conventional delay-and-sum (DAS) beamforming

Given an array of H hydrophones, the output of a general beamformer may be written as

$$z\left[n\right] = \sum_{h=0}^{H-1} w_h^* y_h[n], \tag{1}$$

where n denotes the time sample index, H is the number of hydrophone signals, w_h is the complex weight applied to the h^{th} signal, and $y_h[n]$ is the delayed signal given by

$$y_h[n] = x_h\left[n - f_s\tau_h\right]\exp\left(-\mathrm{j}2\pi f_0\tau_h\right). \tag{2}$$

Here $x_h[n]$ is the complex baseband signal from the h^{th} hydrophone, τ_h is the delay applied to the h^{th} signal, f_s is the sampling frequency, and f_0 is the centre frequency. The beamformer output can be expressed in vector form as

$$\mathbf{z}[n] = \mathbf{w}^H\mathbf{y}[n], \tag{3}$$

where the superscript H denotes the Hermitian transpose. In general, the weight vector $\mathbf{w}$ can be chosen for each time sample.

B. Minimum variance adaptive beamforming

Adaptive beamformers offer improved resolution and noise and interference suppression compared to non-adaptive methods, at the cost of added computational complexity. In contrast to conventional, non-adaptive methods, the apodization weights are not pre-defined. Instead, they are continuously calculated and updated depending on the incoming wavefield. Thus for each pixel in the final image, a different set of weights is used. In this way, the beamformer *adapts* to the data, shaping the beampattern to focus in a given direction while suppressing interfering signals.

Adaptive beamforming is an extension of spectral estimation; the goal being to estimate spatial frequencies closer than the resolution limit of a discrete Fourier transform (DFT). When the echo signals are narrowband there is a direct equivalence between spectral estimation and beamforming since the output signal is just a weighted sum of the (delayed) input signals (equivalent to a FIR filter), as given by (1).

The minimum variance (MV) beamformer is often chosen because of its high resolution capabilities. The MV beamformer is known by many names including the Capon beamformer and the minimum variance distortionless response (MVDR) beamformer. It computes a set of aperture weights to minimize the variance of the output from the beamformer, while ensuring unity gain in the direction of interest. In other words, it lets the signal of interest pass without distortion while at the same time minimizing the variance of the output. The signal of interest in this case is the plane wave arriving from the direction in which we are steering the array. It is assumed that there is only one signal at a time arriving from a given direction. Note that the variance of the output from the beamformer, assuming a zero mean signal, can be expressed as

$$\mathrm{E}\left\{|\mathbf{z}[n]|^2\right\} = \mathrm{E}\left\{|\mathbf{w}^H[n]\mathbf{y}[n]|^2\right\} = \mathbf{w}^H[n]\mathbf{R}[n]\mathbf{w}[n], \quad (4)$$

where $\mathbf{R} = \mathrm{E}\left\{\mathbf{y}\mathbf{y}^H\right\}$ is the spatial covariance matrix. The MV beamformer computes the aperture weights by solving the following minimization problem [9]

$$\arg\min_{\mathbf{w}} \mathbf{w}[n]^H\mathbf{R}[n]\mathbf{w}[n] \text{ subject to } \mathbf{w}[n]^H\mathbf{a}(\tau) = 1, \quad (5)$$

where $\mathbf{w}[n]$ is an $H \times 1$ vector containing the (complex) sensor weights for time sample n, and $\mathbf{a}(\tau)$ is the *steering vector* for a delay τ across the array. When the signals are pre-steered through a time delay in (1), the steering vector is simply a vector of ones. Equation (5) has an analytical solution given by

$$\mathbf{w} = \frac{\mathbf{R}^{-1}\mathbf{a}}{\mathbf{a}^H\mathbf{R}^{-1}\mathbf{a}}. \quad (6)$$

In practice, the covariance matrix $\mathbf{R}$ is unknown and must be estimated from the data using assumptions of ergodicity.

C. Sub-band processing

The MV beamformer was originally developed for narrow-band scenarios. Results from medical ultrasound where the fractional bandwidth is about 50 to 60 percent show that good results can be achieved even in the broadband case as long as the pre-steering time delay in (1) is applied [10]. However, this is only suitable for quasi-narrowband signals since it makes it difficult for an adaptive beamformer to steer the beampattern away from the pre-steered direction to place nulls in directions of interference and thus maximise the SINR.

For broadband signals one can either adapt a FIR filter for each echo signal, as is done in the Frost beamformer [11], or use sub-banding techniques where a vector of complex weights is used for each frequency sub-band. For this paper we have chosen the latter approach.

The echo signals can be sub-banded using a DFT or a polyphase filter bank. This converts the sample data vector $\mathbf{x}$ to $\mathbf{X}_k$, where k is the sub-band frequency index. The beamformer output in each sub-band is then found by applying a set of frequency dependent complex weights $\mathbf{w}_k$,

$$z_k = \mathbf{w}_k^H\mathbf{X}_k. \quad (7)$$

The weights in each sub-band need to be chosen with the constraint that

$$\mathbf{w}_k^H(\tau)\mathbf{a}_k(\tau) = 1. \quad (8)$$

This ensures that the gain in the direction selected by τ is unity. τ is the interferometric delay between the outermost phase centres for an incident plane wave with incident elevation angle θ, where

$$\tau = \frac{d\sin\theta}{c}, \quad (9)$$

Here d is the baseline between the outermost phase centres and c is the speed of propagation. τ can be related to the interferometric phase ϕ_k by

$$\phi_k = 2\pi f_k\tau, \quad (10)$$

where f_k is the sub-band frequency. The vector $\mathbf{a}_k$ in (8) is called the steering vector. It is defined as $\mathbf{a}_k(\tau) = \left[\exp\left(-\mathrm{j}2\pi f_k b_1\tau\right), \exp\left(-\mathrm{j}2\pi f_k b_2\tau\right), \cdots, \exp\left(-\mathrm{j}2\pi f_k b_H\tau\right)\right]^T$ where b_h is the position of the h^{th} phase centre normalised to the baseline d.

The MV weight vector for each frequency sub-band is given by

$$\mathbf{w}_k(\tau) = \frac{\hat{\mathbf{R}}_k^{-1}\mathbf{a}_k(\tau)}{\mathbf{a}_k^H(\tau)\hat{\mathbf{R}}_k^{-1}\mathbf{a}_k(\tau)}. \quad (11)$$

This tries to minimize the variance of the beamformer output subject to the constraint imposed by (8). An estimate of the sample covariance matrix for each sub-band is found by averaging L pings,

$$\hat{\mathbf{R}}_k[n,p] = \frac{1}{L-1}\sum_{l=-L/2}^{L/2-1}\mathbf{X}_k[n,p+l]\mathbf{X}_k^H[n,p+l]. \quad (12)$$

Here n denotes the time sample index n and p is the ping index (these are dropped in the following equations for clarity when appropriate). In practice, the sample mean is removed first. Also, diagonal loading is employed to ensure that the estimated covariance matrix is not singular [12]. The estimated beamformer output variance in sub-band k is

$$\hat{\sigma}_k^2(\tau) = \frac{1}{L-1}\sum_{l=-L/2}^{L/2-1}\left|z_k[p+l] - \bar{z}_k[p+l]\right|^2, \quad (13)$$

where $\bar{z}_k$ is the mean beamformer output for sub-band k and ping p. When using the MV weights,

$$\hat{\sigma}_k^2(\tau) = \frac{1}{\mathbf{a}_k^H(\tau)\hat{\mathbf{R}}_k^{-1}\mathbf{a}_k(\tau)}, \quad (14)$$

Summing the variance over the sub-bands results in

$$\hat{\sigma}^2(\tau) = \sum_{k=1}^{K}\hat{\sigma}_k^2(\tau). \quad (15)$$

(This is equivalent to the beamformer output power when the signals are zero mean.) From this the interferometric delay can be estimated by searching over a number of delays, τ, and choosing the one which maximizes $\hat{\sigma}^2$, i.e.,

$$\begin{aligned}\hat{\tau} &= \arg\max_{\tau}\hat{\sigma}^2(\tau), & (16)\\ &= \arg\max_{\tau}\sum_{k=1}^{K}\frac{1}{\mathbf{a}_k^H(\tau)\hat{\mathbf{R}}_k^{-1}\mathbf{a}_k(\tau)}. & (17)\end{aligned}$$

By comparison, when using a non-adaptive beamformer with fixed weights $\mathbf{w} = [1, 1, \cdots, 1]^T/H$, the interferometric delay estimate is given by

$$\hat{\tau} = \arg\max_{\tau}\sum_{k=1}^{K}\mathbf{a}_k^H(\tau)\hat{\mathbf{R}}_k\mathbf{a}_k(\tau). \quad (18)$$

Using this instead of (17) can be shown equivalent to the maximum likelihood estimator assuming a single angle of arrival, zero mean signals, and an additive noise model [13].

D. Beam steering and selection

Our goal is to find the angle of arrival of the direct-path echo impinging on the array at each instant to reconstruct a bathymetric image as accurately as possible. Because we are operating at shallow depths (less than 20 m), the direction of arrival of the desired signal varies substantially with range as illustrated by Figure 2.

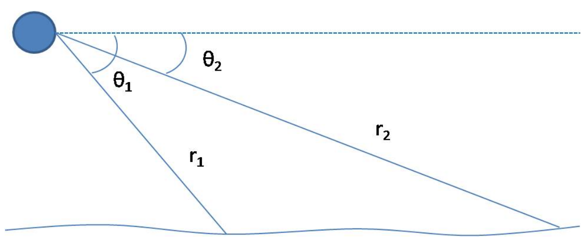

Fig. 2. An example of how the angle of arrival of the desired signal varies with range. A plane wave originating from range r_1 arrives from the direction θ_1 while another plane wave originating from another range, r_2 arrives from the direction θ_2.

If the sea floor is flat this could be accounted by computing a range-dependent angle of arrival defined by simple geometrical observations. However, since the sea floor is not flat, a search is required to find the most likely angle of arrival of the desired signal. For each range sample, the beam is steered to focus in a number of directions covering all the likely angles of arrival. The range of angles to search over can be limited if the approximate expected height variations are known. In our case we have used an educated guess that the sea floor lies between 3 and 10 metres below the sea surface. For each range sample, a number of beams were formed to cover the appropriate angles of arrival. Consecutively steering the beam in each of these directions, the angle of arrival of the signal is assumed to be the "loudest" echo, or the one corresponding to the peak value of the power spectrum of each beamformer. After performing a coarse search, an optimisation routine was used to find the peak response.

IV. Results

Experimental data from the KiwiSAS-4 synthetic aperture sonar, developed by the Acoustics Research Group at the University of Canterbury, were used for this paper [13]. The data were acquired from a sea trial of the KiwiSAS-4 sonar in late January 2006 [13]. The feature of interest is called Parson's Rock—a basalt protrusion 5 m proud of the mud of Lyttelton Harbour, New Zealand. The kiwiSAS-4 sonar is designed to transmit at two centre frequencies simultaneously; 30 kHz and 100 kHz. The results presented in this section are from the frequency band centred at 30 kHz. During the trial, the projector was steered down by 12° in an attempt to reduce the multipath signals resulting from the transmitted signal being reflected from the sea-surface. On the day of the trial the sea was remarkably smooth for a summer's day and this gave rise to noticeable sea-surface multipath as shown in Figure 3, the amplitude of the 30 kHz image for the top hydrophone array.

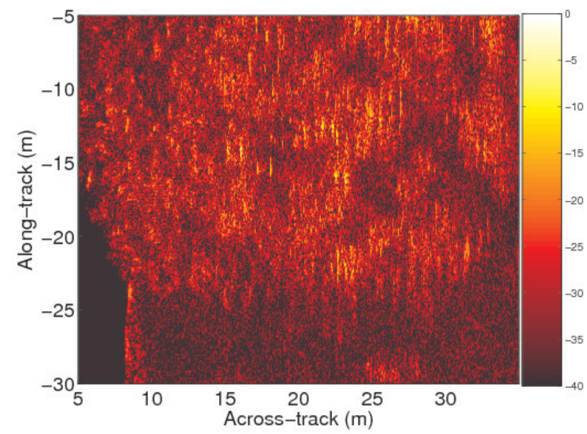

Fig. 3. The reconstructed image from the top hydrophone for the 30 kHz frequency band. The corresponding images from the other array elements are similar.

An example of the beamformer output for a single slant range sample and a single ping, using the conventional and the MV beamformers, respectively, is shown in Figure 4. The beamformer output is plotted as a function of the steering angle. The peak value within this region is assumed to correspond to the direction of arrival of the desired direct echo. As expected, the MV beamformer displays a narrower response than the conventional DAS beamformer.

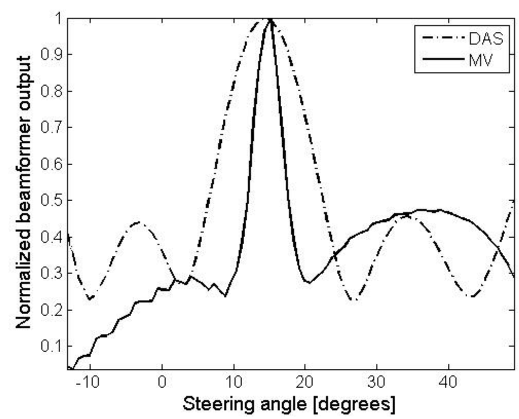

Fig. 4. Beamformer output for the MV and DAS beamformers, for a single ping and a single slant range sample, using experimental data from the KiwiSAS-4. The outputs are plotted as a function of steering angle. The peak corresponds to the angle of arrival estimate.

Figure 5(a) shows the bathymetric image reconstructed using non-adaptive weights. Here (18) was used to find the most likely delay $\hat{\tau}$ for each image pixel and this was mapped to seafloor height using the slant range and known baseline d between the outermost phase centres of the array. $K = 9$ subbands were employed with averaging over $L = 5$ pings. Pixels where the signal power is below the average noise power are coloured black. The corresponding power image is shown in Figure 5(b); this is an image of σ^2 given by (15) at the estimated delay $\hat{\tau}$.

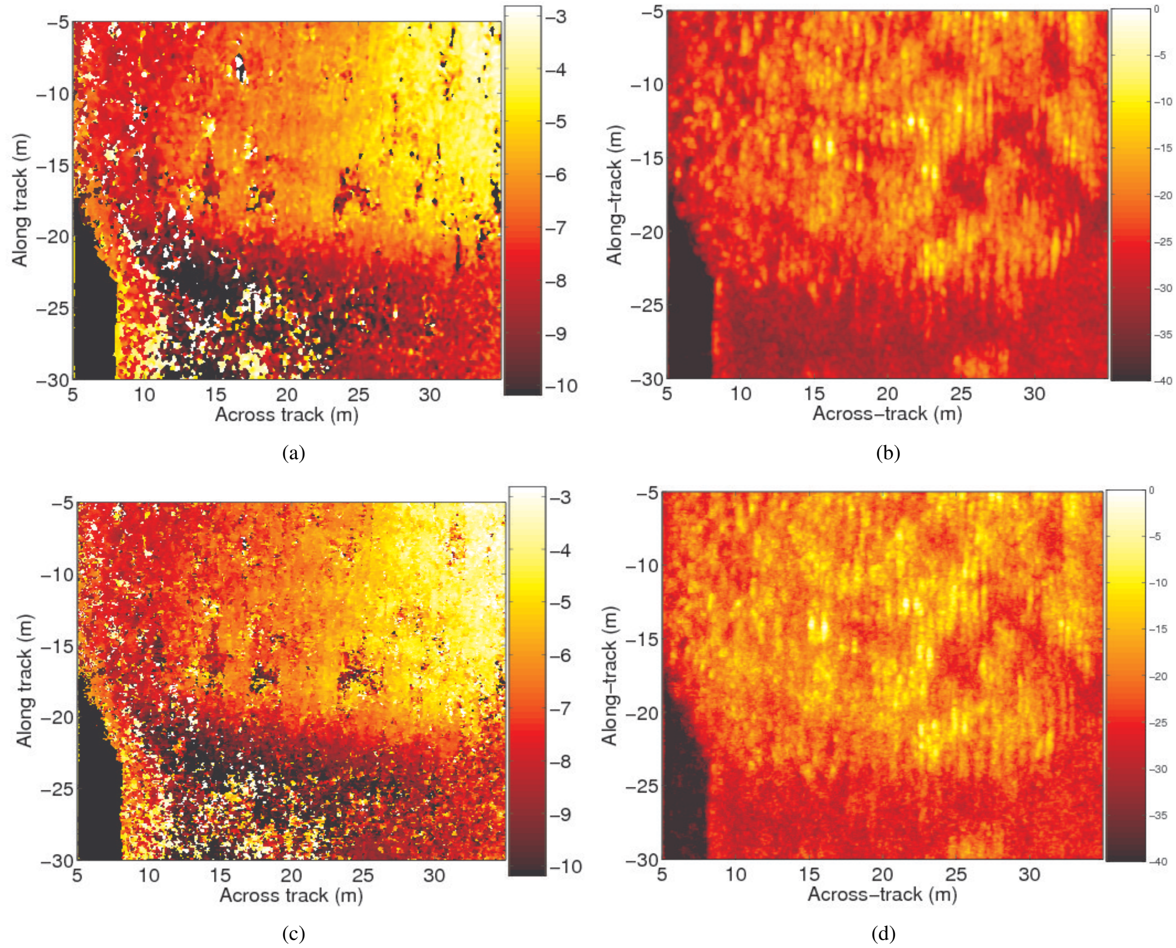

Fig. 5. Reconstructed images for the 30 kHz band: (a) bathymetric image reconstructed using non-adaptive weights; (b) the corresponding power image; (c) bathymetric image reconstructed using MV weights; (d) the corresponding power image.

Figure 5(c) shows the bathymetric image reconstructed using (17) with the MV weights given by (11) and with 1% diagonal loading of the covariance matrix. The corresponding power image is shown in Figure 5(d).

The bathymetric images reconstructed using conventional non-adaptive DAS beamforming and adaptive MV beamforming appear similar. Looking at the power images it appears to be quite a lot of multipath interference left despite our attempts to suppress it using adaptive beamforming. The results are discussed further in Section V.

V. Discussion

Using an array of multiple vertically displaced hydrophones, conventional or adaptive beamforming may be a used to form several beams for a single ping, making it possible to resolve scatterers at the same slant-range but at different heights. Adaptive beamformers such as the MV beamformer in general offer improved resolution as well as the ability of suppressing multipath interference. However, preliminary results using data from the KiwiSAS-4 indicate that the improvement of using adaptive methods for bathymetry is limited. There can be several reasons for this.

Firstly, the data we have used was collected in the Lyttelton Harbour at very shallow depths (about 3–10 m). The shallow water depth combined with the fact that the height of the sea floor varies substantially gives rise to a many possible multiple paths. Our assumption that the dominating multipath is the sea-surface multipath arriving at an angle far from the desired signal, as in Figure 1, might not be valid. In fact, most of the multipath appears to be due to the transmitted signal being reflected from the sea surface and scattering back at similar angles to the direct sea floor reflections.

Another issue may be the way in which we use the MV beamformer to search for the direct path echo. Although the MV beamformer has a higher resolution capability than the conventional beamformer as illustrated by Figure 4, it will struggle if there is an interfering signal arriving from a similar angle as the direct echo. Our search algorithm finds the highest peak within the defined search region and assumes that this corresponds to the angle of arrival of the direct echo. If, however, there is a multipath reflection within the search region which happens to have a higher peak than the direct echo, the beamformer will be steered toward the interfering signal instead of the desired one. In this case the

MV beamformer will attempt to suppress the desired echo.

The MV beamformer is limited by the number of hydrophones in the array since the number of degrees of freedom depends on the size of the weight vector, $\mathbf{w}$. Using one degree of freedom to unsure unity gain in the direction of interest leaves us with the possibility to place only two nulls in the beampattern in an attempt to suppress interfering signals.

It is also worth noting that adaptive beamforming methods are sensitive to the data; in particular good estimates of the covariance matrix are required to make the methods robust. While diagonal loading helps to ensure that the covariance matrix is invertible it also broadens the response, thereby reducing the obtainable resolution. Averaging over several data samples when computing the covariance matrix also adds robustness, but again at the cost of a slightly wider response. As the amount of diagonal loading and averaging increases, the performance of the MV beamformer becomes similar to that of the conventional beamformer.

An alternative beamforming approach which combines the high resolution capabilities of the MV beamformer with the more robust amplitude estimates of the amplitude and phase estimation (APES) beamformer was suggested by Jakobsson et. al. [14]. This suggests using the Capon amplitude spectrum instead of the Capon power spectrum as the frequency estimator. However, our preliminary investigations have shown much poorer reconstructions. This is probably due to coherent interference producing a less smooth spectrum in the region of the desired response.

VI. Conclusion

We have applied conventional as well as adaptive beamforming techniques to experimental SAS-reconstructed data, collected using the KiwiSAS-4 synthetic aperture sidescan sonar. The direction of arrival of the received echo was estimated for each slant range and used to reconstruct the bathymetry. A slight sharpening of the image in the range direction can be observed when using the MV beamformer. However, further studies and simulations are required to fully understand the possibilities and limitations of using adaptive beamforming to suppress some of the multipath interference.

References

[1] M. P. Hayes and P. T. Gough. Synthetic aperture sonar: a review of current status. *IEEE J. Ocean. Eng.*, 34(3):207–224, July 2009.

[2] M. A. Masnadi-Shirazi, D. de Moustier, P. Cervenka, and S. H. Zisk. Differential phase estimation with the SeaMARC II bathymetric sidescan sonar system. *IEEE J. Oc. Eng.*, 17(3):239–251, 1992.

[3] M. P. Hayes, A. J. Hunter, P. J. Barclay, and P. T. Gough. Estimating layover in broadband synthetic aperture sonar bathymetry. In *MTS/IEEE OCEANS'05 Europe*, Brest, France, June 2005.

[4] F. Lombardini, M. Montanari, and F. Gini. Reflectivity estimation for multibaseline interferometric radar imaging of layover extended sources. *IEEE Transactions on Signal Processing*, June 2003.

[5] M. Pinto, A. Bellettini, L. S. Wang, P. Munk, V. Myers, and L. Pautet. A new synthetic aperture sonar design with multipath mitigation. In *Proc. High-Frequency Ocean Acoustics Conf*, volume 728, pages 489–496, La Jolla, CA, USA, 2004.

[6] B. Zerr, L. Goanvic, B. Le Breton, and C. Genty. Bathymetric sidescan sonar: a system dedicated to rapid environment assessment. *Oceans*, 2005.

[7] X. Lurton. Swath bathymetry using phase difference: Theoretical analysis of acoustical measurement precision. *IEEE J. Ocean. Eng.*, 25(3):351–363, July 2000.

[8] M. P. Hayes. Multipath reduction with a three element interferometric synthetic aperture sonar. In *Proc. Seventh Euro. Conf. Underwater Acoust. (ECUA)*, pages 1151–1156, Delft, The Netherlands, July 2004. ECUA.

[9] J. Capon. High-resolution frequancy-wavenumber spectrum analysis. *Proc. IEEE*, pages 1408–1418, August 1969.

[10] J.-F. Synnevåg, A. Austeng, and S. Holm. Adaptive beamforming applied to medical ultrasound imaging. *IEEE Trans. Ultrason., Ferroelec., Freq. Contr.*, pages 1606–1613, August 2007.

[11] O. L. Frost. An algorithm for linearly constrained adaptive array processing. *Proc. IEEE*, 60:926–935, 1972.

[12] J.Li, P. Stoica, and Z. Wang. On robust capon beamforming and diagonal loading. 51(7):1702–1715, 2005.

[13] M. P. Hayes. Results of a multiple-baseline interferometric synthetic aperture sonar in shallow water. In *IVCNZ'06, Image and Vision Computing New Zealand*, pages 287–292, Great Barrier Island, New Zealand, 2006.

[14] A. Jakobsson and P. Stoica. Combining Capon and APES for estimation of spectral lines. *Circuits Systems Signal Process*, 19(2):159–169, 2000.